

LETTER TO THE EDITOR

# A method to measure CO and N<sub>2</sub> depletion profiles inside prestellar cores<sup>★</sup>

L. Pagani<sup>1</sup>, A. Bourgoïn<sup>1</sup>, and F. Lique<sup>2,1</sup>

<sup>1</sup> LERMA, UMR8112 du CNRS, Observatoire de Paris, 61, Av. de l'Observatoire, 75014 Paris, France.  
e-mail: laurent.pagani@obspm.fr

<sup>2</sup> LOMC - UMR 6294, CNRS-Université du Havre 25 rue Philippe Lebon CS 80540 - 76 058 Le Havre cedex

Received 31/07/2012; 01/11/2012

## ABSTRACT

**Context.** In the dense and cold prestellar cores, many species freeze out onto grains to form ices. The most conspicuous case is that of CO itself. Only upper limits of this depletion amplitude can be estimated because the CO emission from the external undepleted layers mask the emission of CO left inside the depleted region. The finite signal-to-noise ratio of the observations is another limitation. However, depletion and even more desorption mechanisms are not well-known and need observational constraints, i.e., depletion profiles.

**Aims.** We describe a method for retrieving the CO and N<sub>2</sub> abundance profiles inside prestellar cores, which is mostly free from initial conditions.

**Methods.** DCO<sup>+</sup> is a daughter molecule of CO, which appears inside depleted prestellar cores. The main deuteration partners are the H<sub>3</sub><sup>+</sup> isotopologues. By determining the abundance of these isotopologues via N<sub>2</sub>D<sup>+</sup>, N<sub>2</sub>H<sup>+</sup>, and ortho-H<sub>2</sub>D<sup>+</sup> observations and a chemical model, we can uniquely constrain the CO abundance, the only free parameter left, to fit the observed DCO<sup>+</sup> abundance. The N<sub>2</sub> abundance is also determined in the same manner once CO is known. DCO<sup>+</sup>-H<sub>2</sub> collisional rates including the hyperfine structure were computed in order to determine the DCO<sup>+</sup> abundance.

**Results.** To illustrate the method, we apply it to the main L183 prestellar core and find that the CO abundance profile varies from  $\geq 2.4 \times 10^{-5}$  at the core edge to  $\leq 6.6 \times 10^{-8}$  at the center. This represents a relative decrease in abundance by  $\geq 360$ , and by  $\geq 2000$  compared to the standard undepleted CO abundance ( $1-2 \times 10^{-4}$ ). Comparatively, N<sub>2</sub> abundance decreases much less, from  $\leq 3.7 \times 10^{-7}$  down to  $\sim 2.9 \times 10^{-8}$ , in contrast to the similar binding properties of the two species. Because the N<sub>2</sub> abundance is lower than its steady state value at the edge, while CO is close to its own, a possible explanation is that N<sub>2</sub> is still in its production phase in competition with depletion.

**Conclusions.** The method allows the CO and N<sub>2</sub> abundance profiles to be retrieved in the depleted zone both without needing extremely high signal-to-noise observations and free of masking effects by extended emission from the cloud envelope. The main uncertainties are linked to the N<sub>2</sub>H<sup>+</sup> collisional rates and somewhat to the H<sub>3</sub><sup>+</sup> isotopologue rates, both collisional and chemical, but hardly to the initial conditions of the model. This method opens up possibilities testing depletion and desorption mechanisms in prestellar cores and time evolution models, and of addressing the debated CO/N<sub>2</sub> depletion controversy.

**Key words.** ISM: abundances — ISM: clouds — evolution — ISM: molecules — astrochemistry — ISM: individual objects : L183

## 1. Introduction

Stars form inside dark clouds consisting of large amounts of gas and dust at low temperatures ( $\sim 10$  K). Isolated low-mass star formation is presently well-understood qualitatively, but several steps are still unclear or need quantification. One such step is the formation of prestellar cores inside the clouds. Prestellar cores (hereafter PSCs) are cores with densities above  $1 \times 10^5 \text{ cm}^{-3}$  (Keto & Caselli 2008) into which heavy gaseous species are usually depleted, i.e., molecules such as CO, CS, SO, stick to the grains and become ices. Much work has been devoted to the depletion phenomenon since its initial discovery (Lemme et al. 1995, though its possible existence was already invoked in early papers such as Herbst & Klemperer 1973), which followed soon after the arrival of the first submillimeter bolometers that were able to uncover the cold and dense PSCs (Ward-Thompson et al. 1994). Depletion has been detected in many cold cores since

then (e.g., Willacy et al. 1998; Caselli et al. 1999; Tafalla et al. 2002, 2004; Pagani et al. 2005; Brady-Ford & Shirley 2011) with only a very few counterexamples of very dense and cold cores not showing depletion (e.g., L1521E, Tafalla & Santiago 2004). Though depletion usually starts to appear in cores when extinction becomes higher than  $\sim 8 A_V$  and densities  $n > 3 \times 10^4 \text{ cm}^{-3}$ , when looking at the different papers cited above, there are also cases of strong depletion in cores that are not yet prestellar like L1498 (Willacy et al. 1998), L1506C (Pagani et al. 2010), and TMC2 (Brady-Ford & Shirley 2011). The reason is not yet clear.

Though CO is the main species used to reveal depletion, many others are known to deplete. Water is probably the first one to deplete when penetrating the clouds owing to its H-bond capability and consequently high sublimation temperature (but is also difficult to study). Other species, such as CS and SO, have been shown to deplete (e.g. Tafalla et al. 2002, 2004; Pagani et al. 2005). A controversy has arisen about the remarkable resistance of N-bearing species to not depleting and their column density to being, on first order, proportional to the amount of dust. Such is the case for NH<sub>3</sub>, CN, HCN, and N<sub>2</sub>H<sup>+</sup>. For NH<sub>3</sub>,

<sup>★</sup> Based on observations carried out with the IRAM 30m Telescope. IRAM is supported by INSU/CNRS (France), MPG (Germany), and IGN (Spain).

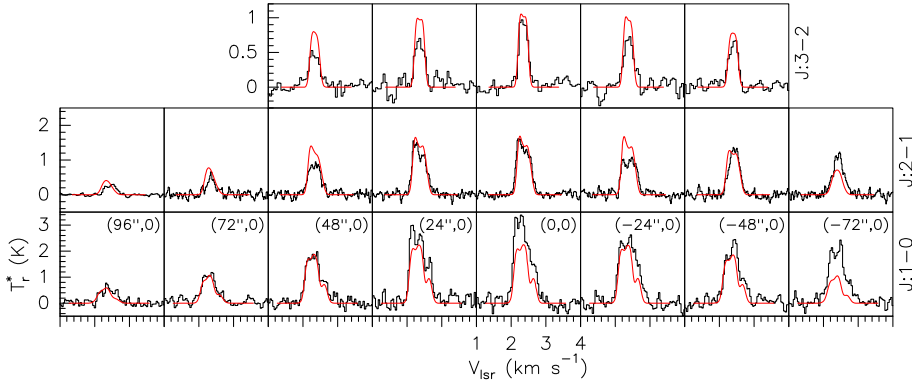


**Fig. 1.** DCO<sup>+</sup> observations (histogram) and fit (red line) for J:1-0 (bottom line), J:2-1 (middle line), and J:3-2 (top line) across L183 main PSC. Offsets are indicated for the J:1-0 transition and apply to all. The cut, though sparsely sampled for the J:2-1 and J:3-2 lines, is along the same N<sub>2</sub>H<sup>+</sup> cut as in Paper I and crosses the dust peak.

Tafalla et al. (2002, 2004) even show an increase in abundance in the prestellar core centers, while N<sub>2</sub>H<sup>+</sup> abundance seems to be constant with radius. The absence of depletion for CN and HCN has been reported by Hily-Blant et al. (2008, 2010). A few works indicate possible depletion of N<sub>2</sub>H<sup>+</sup> (Bergin et al. 2002; Belloche & André 2004; Di Francesco et al. 2004), and Pagani et al. (2007, hereafter Paper I) USE a detailed radiative transfer modeling of L183 to show that N<sub>2</sub>H<sup>+</sup> starts to decrease in abundance above  $n \approx 5 \times 10^5 \text{ cm}^{-3}$ , a possible sign of the depletion of its parent species N<sub>2</sub> above that density. However, the reason for this late depletion of N<sub>2</sub> compared to that of CO is not clear, since both species have the same weight, one is apolar, the other weakly polar, and therefore should have approximately comparable behaviors in terms of freezing-out and desorption mechanisms. Despite their similarity, chemical models have tried to reproduce the different behaviors of both species by supposing different binding energies (e.g. Bergin & Langer 1997; Bergin et al. 2002), but laboratory work has shown that this is not correct (Öberg et al. 2005; Bisschop et al. 2006; Öberg et al. 2009) so the problem persists. Because both DCO<sup>+</sup> and the pair (N<sub>2</sub>H<sup>+</sup>, N<sub>2</sub>D<sup>+</sup>) are observed in depleted cores, one possible explanation is that CO and N<sub>2</sub> both deplete in similar proportions, but since their relative abundances to H<sub>2</sub> before depletion are very high ( $X[\text{CO}] = \text{CO}/\text{H}_2 \approx 1 \times 10^{-4}$  and possibly  $X[\text{N}_2] \approx 1 \times 10^{-5}$ ), enough molecules remain, even for a factor 1000 depletion, to produce these daughter species to their observed abundances (typically in the range  $1 \times 10^{-11} - 1 \times 10^{-10}$ ). However, observations of N<sub>2</sub> itself are impossible because of the lack of a dipole moment, which prevents emission in the radio domain, and CO emission in the core is masked by the strong CO lines emitted in the undepleted parts of the cloud. This is true for all CO isotopologues. Since CO is easily thermalized in clouds, even their envelope shines strongly in the low rotational transitions, and column density fluctuations (the envelope is certainly not a regular sphere of constant thickness) do not allow retrieval of the CO abundance inside the core. Another limitation comes from the finite signal-to-noise ratio of observed spectra. To detect a variation of 10% in intensity, a signal-to-noise ratio of 30 would be required and that would hardly be sufficient to separate an abundance drop of 100 from one of  $10^3$  (though such an attempt has been made recently, Brady-Ford & Shirley 2011, but the authors do conclude that they cannot distinguish between a depletion factor of 10 or of 1000).

Based on the fact that DCO<sup>+</sup> is a daughter species of CO and that it is present almost only in the depleted core (unlike the other HCO<sup>+</sup> isotopologues, see Pagani et al. 2011), we propose to retrieve the abundance profile of CO where it depletes. Measuring DCO<sup>+</sup> alone would imply having to rely entirely on a chemical model to retrieve CO. Here, we propose to take advantage of the measurement of three other species, N<sub>2</sub>H<sup>+</sup>, N<sub>2</sub>D<sup>+</sup>, and H<sub>2</sub>D<sup>+</sup>,

which are also confined to the prestellar core, to strongly constrain the deuteration enrichment process of DCO<sup>+</sup> and therefore constrain the CO abundance itself. We simply have to exploit the model presented in Pagani et al. (2009, hereafter Paper II) and adjust it to explain all four observed species. The outcome is the N<sub>2</sub> and CO abundance profiles across the core.

In Sect. 2, we present the DCO<sup>+</sup> observations of one test case, the L183 prestellar core, and in Sect. 3 their radiative transfer modeling. Section 4 presents the method for constraining the CO and N<sub>2</sub> abundances from the observations of daughter species. We discuss their depletion profiles in L183 and present our conclusions in Sect. 5. DCO<sup>+</sup>-H<sub>2</sub> collisional rates are presented in an online appendix.

## 2. Observations

We observed DCO<sup>+</sup> (J:1-0), (J:2-1), and (J:3-2) lines with the IRAM - 30m from 12 to 14 July 2008. For the (J:1-0) transition, the image rejection was relatively low, the receiver being somewhat outside the original range of frequencies for which it was designed and close to the low side cutoff-frequency. Therefore the image/signal gain ratio was measured after the tuning and found to be 0.73. The other lines benefited from standard tunings with gain ratios of only 0.03. The sky was reasonably good. Zenithal opacity was 0.15, 0.1, and 0.3 for the (J:1-0), (J:2-1), and (J:3-2) lines, respectively and the system temperature of the order of 400, 200, and 450 K (in the T<sub>a</sub><sup>\*</sup> scale, similar to the T<sub>r</sub><sup>\*</sup> scale for this telescope, see Pagani et al. 2005). We used the versatile autocorrelator as a backend (VESPA) with resolutions of 10, 10, and 40 kHz, respectively, corresponding to velocity resolutions of 41, 20, and 54 m s<sup>-1</sup> with bandwidths of 40, 20, and 40 MHz. The spatial resolution is 36, 18, and 12'', respectively. Observations were done in frequency-switch mode. The pointing and focus were checked. The pointing accuracy remained within 3''.

The N<sub>2</sub>H<sup>+</sup> and N<sub>2</sub>D<sup>+</sup> observations were described and analyzed in Paper I, while the ortho-H<sub>2</sub>D<sup>+</sup> data are presented and analyzed in Paper II. The reference position is  $\alpha(2000) = 15\text{h}54\text{m}08.5\text{s}$ ,  $\delta(2000) = -2^\circ 52' 48''$ .

## 3. Analysis

For DCO<sup>+</sup>, we performed only two short perpendicular cuts: one vertical, along the dense filament, and one perpendicular to it, with 24'' spacings. Only the horizontal cut is displayed in Fig. 1. As for N<sub>2</sub>H<sup>+</sup>, N<sub>2</sub>D<sup>+</sup>, and ortho-H<sub>2</sub>D<sup>+</sup>, the line intensities peak toward the prestellar core and are approximately constant along the ridge. They strongly decrease away from it to the left (east). The decrease is not as strong to the right (west) because a secondary dust peak lies slightly farther away in that direction

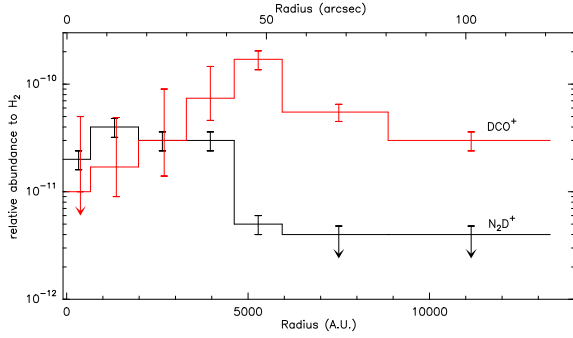


**Fig. 2.** DCO<sup>+</sup> relative abundance (in volume) from the radiative transfer fit of the observations (in red). N<sub>2</sub>D<sup>+</sup> abundance (from Paper I, Table 2) is also displayed. The x axis is cylindrical radius referring to Fig. 1.

(see Pagani et al. 2004). Due to its hyperfine structure (hereafter HFS, Caselli & Dore 2005), the (J:1–0) line is markedly wider (0.54 km s<sup>-1</sup>) than the (J:2–1) line (0.44 km s<sup>-1</sup>), itself wider than the (J:3–2) line (0.3 km s<sup>-1</sup>) and all of them being wider than the N<sub>2</sub>D<sup>+</sup> and N<sub>2</sub>H<sup>+</sup> lines (0.2 km s<sup>-1</sup>). Fitting the lines with the CLASS HFS routine loaded with the description of the DCO<sup>+</sup> HFS structure, we found a velocity width of ~0.2 km s<sup>-1</sup> for each HFS component, in agreement with the N<sub>2</sub>H<sup>+</sup> and N<sub>2</sub>D<sup>+</sup> determinations.

We modeled the DCO<sup>+</sup> emission using the best-fit model of the L183 PSC in density, temperature, and large-scale velocity (see Paper I, their Table 2) and the same spherical Monte-Carlo radiative transfer model adapted to HFS treatment, including line overlap as for N<sub>2</sub>D<sup>+</sup> and N<sub>2</sub>H<sup>+</sup> (Paper I). Though recent HFS-resolved DCO<sup>+</sup>–He collisional coefficients have been published (Buffa 2012), we found that it was impossible to fit the observations with the same density and temperature profile as for N<sub>2</sub>H<sup>+</sup>, the modeled lines being far too weak. Instead, we computed new HFS-resolved DCO<sup>+</sup>–H<sub>2</sub> rate coefficients based on those of HCO<sup>+</sup> with para-H<sub>2</sub> from BASECOL (Flower 1999; Dubernet et al. 2006), following the method proposed by Faure & Lique (2012, see Appendix). To compare the model to the observations, we convolved the model output as if it was coming from a cylinder (to mimic the filament) with the 30-m main beam and error beams (as in Paper I). The Monte-Carlo output fit is displayed in Fig. 1 and the resulting DCO<sup>+</sup> abundance fit with its estimated dispersion is displayed in Fig. 2. The only free parameter of the model is the DCO<sup>+</sup> abundance profile. The N<sub>2</sub>D<sup>+</sup> abundance profile (from Paper I, Table 2) is traced in the same figure. While the N<sub>2</sub>D<sup>+</sup> abundance shows only a mild diminution in the PSC center, DCO<sup>+</sup> is clearly more extended than N<sub>2</sub>D<sup>+</sup>, but the central drop is a factor ≥17, almost one order of magnitude more than that of N<sub>2</sub>D<sup>+</sup>.

#### 4. Description of the method

To determine CO abundance from DCO<sup>+</sup> observations, one needs to know the main reaction paths that lead from CO to DCO<sup>+</sup> and the main destruction routes of DCO<sup>+</sup>. Chemical models can perform such an analysis but they depend on initial conditions, some of which are difficult to know, such as the grain size distribution or the cosmic ray ionization rate. In the case of a depleted PSC, the main reactions that form DCO<sup>+</sup> involve CO and the three deuterated H<sub>3</sub><sup>+</sup> isotopologues. With the possible measurement of only one or rarely two of these species, namely ortho-H<sub>2</sub>D<sup>+</sup> and para-D<sub>2</sub>H<sup>+</sup>, too many solutions can be found with various CO abundances to fit the observed DCO<sup>+</sup> abundance. To avoid these uncertainties, we instead consider

the isotopologue ratio DCO<sup>+</sup>/HCO<sup>+</sup>. They both derive mostly from reactions of CO with H<sub>3</sub><sup>+</sup> isotopologues (in depleted cores) and are both destroyed by (mostly) electrons. Therefore the DCO<sup>+</sup>/HCO<sup>+</sup> ratio only depends on the balance between the four H<sub>3</sub><sup>+</sup> isotopologues. CO and e<sup>-</sup> abundances are not needed to determine this balance. Therefore, knowing the abundance of one of the H<sub>3</sub><sup>+</sup> isotopologues and the balance between them, a unique solution of the deuteration enrichment can be found. We also need to know the destruction rate of DCO<sup>+</sup> with the electrons to fix the CO abundance. The e<sup>-</sup> abundance depends primarily on the density and on the cosmic ray ionization rate (Walmsley et al. 2004). In Paper II, the cosmic ray ionization rate (and therefore the e<sup>-</sup> abundance) is not a free parameter (though not mentioned). We had to adjust it to both fit the deuteration balance and the ortho-H<sub>2</sub>D<sup>+</sup> observed abundance at the same moment, and the range of possible values was relatively narrow ( $\zeta = 2-3 \times 10^{-17} \text{ s}^{-1}$ ). Therefore the knowledge of the DCO<sup>+</sup>/HCO<sup>+</sup> ratio and of the ortho-H<sub>2</sub>D<sup>+</sup> abundance allows to constrain uniquely the CO abundance. However, the scheme is not feasible because HCO<sup>+</sup> is spread all over the cloud since CO and H<sub>3</sub><sup>+</sup> are both abundant everywhere. Since the HCO<sup>+</sup> lines are very optically thick, there is no possibility to derive the HCO<sup>+</sup> abundance inside the PSC itself and the DCO<sup>+</sup>/HCO<sup>+</sup> ratio cannot be established. H<sup>13</sup>CO<sup>+</sup> meets the same problem, and HC<sup>18</sup>O<sup>+</sup> is too weak here. Instead, because the DCO<sup>+</sup>/HCO<sup>+</sup> and the N<sub>2</sub>D<sup>+</sup>/N<sub>2</sub>H<sup>+</sup> ratios follow the same chemical scheme inside the PSC (Pagani et al. 2011), and both depend only on the same deuteration balance we use the latter ratio to determine that balance, since both its species are confined to the PSC.

Quantitatively, we ran the same chemical model as in Paper II, and we refer the reader to it for details. However, we slightly modified the reaction network. We introduced the new ortho-H<sub>2</sub> + H<sup>+</sup> ↔ para-H<sub>2</sub> + H<sup>+</sup> reaction rate from Honvault et al. (2011), which shows that this conversion rate is slowed by a factor of 2 compared to the previous value (Gerlich 1990). The effect is to slow down the ortho-to-para H<sub>2</sub> conversion and somewhat increase the time it takes for deuteration processes to become efficient (see Paper II). Recombination of N<sub>2</sub>H<sup>+</sup> with electrons is supposed to give only N<sub>2</sub> + H and not N + NH (see however Hily-Blant et al. 2010, for a different approach and discussion therein). Because these reactions of formation and destruction of HCO<sup>+</sup> and N<sub>2</sub>H<sup>+</sup> are relatively fast (100 years, Parise et al. 2011), we consider that even if other phenomena compete for the CO or for the N<sub>2</sub> resources, like depletion, fitting the observed N<sub>2</sub>H<sup>+</sup>, N<sub>2</sub>D<sup>+</sup>, and DCO<sup>+</sup> local abundances gives the present abundance of the parent molecule, N<sub>2</sub> or CO. To find the CO abundance needed to explain the DCO<sup>+</sup> abundance in the model, we adjust the CO one, until the DCO<sup>+</sup> abundance reaches the observed value at the same moment as the observed N<sub>2</sub>D<sup>+</sup>/N<sub>2</sub>H<sup>+</sup> ratio and ortho-H<sub>2</sub>D<sup>+</sup> abundance are reached, layer after layer (see Paper II, their Fig. 7). Because N<sub>2</sub>H<sup>+</sup> and N<sub>2</sub>D<sup>+</sup> react with CO to form HCO<sup>+</sup> and DCO<sup>+</sup>, respectively, the abundance of N<sub>2</sub> slightly depends upon that of CO and needs to be adjusted after that of CO to reproduce the observed N<sub>2</sub>D<sup>+</sup> and N<sub>2</sub>H<sup>+</sup> abundances. If the edge of the depleted region is reached, we should be able to smoothly connect the CO abundance derived from our modeling with the undepleted CO abundance. However, N<sub>2</sub>D<sup>+</sup> usually disappears before reaching this edge, thus preventing to extend the model that far, and it is possible that abundance jumps exist (Pagani et al. 2010).

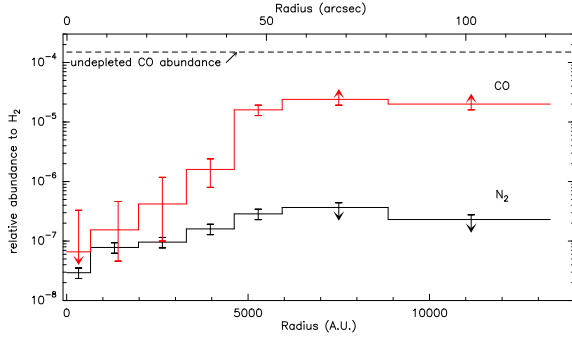


**Fig. 3.** CO and N<sub>2</sub> relative abundances (in volume) derived from the chemical model. The x-axis is cylindrical radius referring to Fig. 1.

## 5. Discussion & conclusion

Figure 3 shows the modeled CO and N<sub>2</sub> abundance profiles in the PSC as a function of distance. Lower limits for CO in the outer parts are due to the upper limit on N<sub>2</sub>D<sup>+</sup> abundance, limiting our knowledge of the H<sub>3</sub><sup>+</sup> isotopologue balance. The upper limit in the center is linked to the DCO<sup>+</sup> upper limit itself. CO abundance starts close to the undepleted abundance ( $1-2 \times 10^{-4}$ , e.g., Dickman 1978; Pineda et al. 2010). It drops by  $\geq 360$  in the PSC and by  $\geq 2000$  compared to the undepleted abundance. This is the first time such a drop has been reported. It is possibly not unique to this source, but this question will be addressed when we have extended this method to other PSCs. It is interesting to note that the CO profile compares favorably with the results of Aikawa et al. (2005), especially their case with a peak density of  $3 \times 10^6 \text{ cm}^{-3}$ , and  $\alpha = 4$  (= fast collapse case, their Fig. 3, middle left) which is close to the L183 PSC conditions.

The N<sub>2</sub> abundance seems to first increase up to  $\leq 3.7 \times 10^{-7}$ , much lower than what it would reach in a chemical model at steady state ( $\sim 1 \times 10^{-5}$ , Flower et al. 2006) but then decreases only by a factor of  $\leq 12$ . This is also the first time that such a profile can be reported and that the CO and N<sub>2</sub> profiles are compared. From the work of Öberg et al. (2005, 2009) and Bisschop et al. (2006), we know that this different behavior cannot be attributed to different adsorption and desorption properties of both species. Because N<sub>2</sub> has not reached its steady state abundance, contrary to CO, it is possible that enough atomic N is still available to keep forming N<sub>2</sub> in the core. Di Francesco et al. (2007) indicate that atomic N has a lower binding energy than N<sub>2</sub> or CO, which would help in this scenario. A possible route to the formation of N<sub>2</sub> from N involves the presence of CN (e.g., Hily-Blant et al. 2010):



Hily-Blant et al. (2008) have shown that CN is not depleted in L183, with an abundance of  $\sim 8 \times 10^{-10}$ . The production rate of N<sub>2</sub> ( $k \times [\text{N}][\text{CN}]$ , with  $k \sim 5 \times 10^{-11} \text{ cm}^3 \text{ s}^{-1}$ , Wakelam et al. 2012, and  $[\text{N}]$  and  $[\text{CN}]$  the density of the species) would therefore be  $1.6 \times 10^{-7} X[\text{N}] \text{ cm}^{-3} \text{ s}^{-1}$  in the center of the PSC (where  $n(\text{H}_2) = 2 \times 10^6 \text{ cm}^{-3}$ ) down to  $4.6 \times 10^{-11} X[\text{N}] \text{ cm}^{-3} \text{ s}^{-1}$  at the edge ( $n(\text{H}_2) = 3.4 \times 10^4 \text{ cm}^{-3}$ ), to be compared to the freeze-out rate (e.g., Bergin & Tafalla 2007),  $[\text{N}_2]k_{\text{fo}} = 2.6 \times 10^{-5} X[\text{N}_2] \text{ cm}^{-3} \text{ s}^{-1}$  at the center and  $7.5 \times 10^{-9} X[\text{N}_2] \text{ cm}^{-3} \text{ s}^{-1}$  at the edge. For the  $X[\text{N}_2]$  values found here, we see that though the depletion rate is low at the edge ( $1.5 \times 10^{-15} \text{ cm}^{-3} \text{ s}^{-1}$ ), the formation rate cannot compensate for any reasonable value of  $X[\text{N}]$  ( $4.6 \times 10^{-16} \text{ cm}^{-3} \text{ s}^{-1}$  for  $X[\text{N}] = 1 \times 10^{-5}$ ). In the center, the depletion rate is much higher ( $8 \times 10^{-13} \text{ cm}^{-3} \text{ s}^{-1}$ ), but the

N<sub>2</sub> production rate is in the range  $1.8 \times 10^{-12} - 10^{-14}$  for  $X[\text{N}] = 1 \times 10^{-5} - 10^{-7}$ ), and therefore comparable. If N is not too depleted in PSCs, combined to the presence of CN, this could explain the slower decrease in N<sub>2</sub> with density than in CO.

The method presented here suffers from two types of uncertainties: on collisional coefficients and on reaction rates. The critical ones are the N<sub>2</sub>H<sup>+</sup>-He collisional coefficients (Daniel et al. 2005) that underestimate the real N<sub>2</sub>H<sup>+</sup>-H<sub>2</sub> ones and the ortho-H<sub>2</sub>D<sup>+</sup>-H<sub>2</sub> collisional coefficients that are needed to retrieve the ortho-H<sub>2</sub>D<sup>+</sup> abundance (from Hugo et al. 2009). Therefore, the abundance profiles of DCO<sup>+</sup>, N<sub>2</sub>D<sup>+</sup> (both depending on the temperature and density profiles derived from N<sub>2</sub>H<sup>+</sup>), and ortho-H<sub>2</sub>D<sup>+</sup> remain tentative and were presented mostly to illustrate the method until new collisional coefficients become available. Less important, because the deuteration is constrained by the N<sub>2</sub>D<sup>+</sup>/N<sub>2</sub>H<sup>+</sup> ratio, are the reaction rates of the H<sub>3</sub><sup>+</sup> network (evaluated statistically by Hugo et al. 2009).

The simple approach we propose here allows deriving the CO and N<sub>2</sub> abundances in PSCs and tracing their profile without any strong dependence upon the initial conditions and with good precision, though it is still limited at the moment by uncertain coefficients and rates. The obtention of these profiles will allow to address several pending problems such as the determination of the efficient processes to desorb molecules in PSCs, time-evolution of PSCs based on their depletion profiles and the CO/N<sub>2</sub> differential depletion crisis.

*Acknowledgements.* We are grateful to F. Daniel for providing us with the frequencies and  $A_{ij}$ s of the DCO<sup>+</sup> HFS, to P.F. Goldsmith for useful references, and to an anonymous referee who helped us to clarify and improve the manuscript.

## References

- Aikawa, Y., Herbst, E., Roberts, H., & Caselli, P. 2005, *ApJ*, 620, 330  
Alexander, M. H. & Dagdigan, P. J. 1985, *J. Chem. Phys.*, 83, 2191  
Belloche, A. & André, P. 2004, *A&A*, 419, L35  
Bergin, E. A., Alves, J., Huard, T., & Lada, C. J. 2002, *ApJ*, 570, L101  
Bergin, E. A. & Langer, W. D. 1997, *ApJ*, 486, 316  
Bergin, E. A. & Tafalla, M. 2007, *ARA&A*, 45, 339  
Bisschop, S. E., Fraser, H. J., Öberg, K. I., van Dishoeck, E. F., & Schlemmer, S. 2006, *A&A*, 449, 1297  
Brady-Ford, A. & Shirley, Y. L. 2011, *ApJ*, 728, 144  
Buffa, G. 2012, *MNRAS*, 421, 719  
Caselli, P. & Dore, L. 2005, *A&A*, 433, 1145  
Caselli, P., Walmsley, C. M., Tafalla, M., Dore, L., & Myers, P. C. 1999, *ApJ*, 523, L165  
Corey, G. C. & McCourt, F. R. 1983, *J. Phys. Chem.*, 87, 2723  
Daniel, F., Dubernet, M.-L., Meuwly, M., Cernicharo, J., & Pagani, L. 2005, *MNRAS*, 363, 1083  
Di Francesco, J., André, P., & Myers, P. C. 2004, *ApJ*, 617, 425  
Di Francesco, J., Evans II, N. J., Caselli, P., et al. 2007, *Protostars and Planets V*, 17  
Dickman, R. L. 1978, *ApJS*, 37, 407  
Dubernet, M.-L., Grosjean, A., Flower, D., et al. 2006, *Journal of Plasma Research Series*, Volume 7, p. 356-357, 7, 356  
Faure, A. & Lique, F. 2012, *MNRAS*, 425, 740  
Flower, D. R. 1999, *MNRAS*, 305, 651  
Flower, D. R., Pineau Des Forêts, G., & Walmsley, C. M. 2006, *A&A*, 456, 215  
Gerlich, D. 1990, *JCP*, 92, 2377  
Herbst, E. & Klemperer, W. 1973, *ApJ*, 185, 505  
Hily-Blant, P., Walmsley, M., Pineau Des Forêts, G., & Flower, D. 2008, *A&A*, 480, L5  
Hily-Blant, P., Walmsley, M., Pineau Des Forêts, G., & Flower, D. 2010, *A&A*, 513, A41  
Honvault, P., Jorfi, M., González-Lezana, T., Faure, A., & Pagani, L. 2011, *Physical Chemistry Chemical Physics*, 13, 19089  
Hugo, E., Asvany, O., & Schlemmer, S. 2009, *JCP*, 130, 164302  
Keto, E. & Caselli, P. 2008, *ApJ*, 683, 238  
Lemme, C., Walmsley, C. M., Wilson, T. L., & Muders, D. 1995, *A&A*, 302, 509  
Lique, F., Toboła, R., Kłos, J., et al. 2008, *Astron. Astrophys.*, 478, 567

- Neufeld, D. A. & Green, S. 1994, *ApJ*, 432, 158
- Öberg, K. I., van Broekhuizen, F., Fraser, H. J., et al. 2005, *ApJ*, 621, L33
- Öberg, K. I., van Dishoeck, E. F., & Linnartz, H. 2009, *A&A*, 496, 281
- Pagani, L., Bacmann, A., Cabrit, S., & Vastel, C. 2007, *A&A*, 467, 179, Paper I
- Pagani, L., Bacmann, A., Motte, F., et al. 2004, *A&A*, 417, 605
- Pagani, L., Pardo, J.-R., Apponi, A. J., Bacmann, A., & Cabrit, S. 2005, *A&A*, 429, 181
- Pagani, L., Ristorcelli, I., Boudet, N., et al. 2010, *A&A*, 512, A3
- Pagani, L., Roueff, E., & Lesaffre, P. 2011, *ApJ*, 739, L35
- Pagani, L., Vastel, C., Hugo, E., et al. 2009, *A&A*, 494, 623, Paper II
- Parise, B., Belloche, A., Du, F., Güsten, R., & Menten, K. M. 2011, *A&A*, 526, A31
- Pineda, J. L., Goldsmith, P. F., Chapman, N., et al. 2010, *ApJ*, 721, 686
- Tafalla, M., Myers, P. C., Caselli, P., & Walmsley, M. 2004, *A&A*, 416, 191
- Tafalla, M., Myers, P. C., Caselli, P., Walmsley, M., & Comito, C. 2002, *ApJ*, 569, 815
- Tafalla, M. & Santiago, J. 2004, *A&A*, 414, L53
- Wakelam, V., Herbst, E., Loison, J.-C., et al. 2012, *ApJS*, 199, 21
- Walmsley, C. M., Flower, D. R., & Pineau des Forêts, G. 2004, *A&A*, 418, 1035
- Ward-Thompson, D., Scott, P. F., Hills, R. E., & André, P. 1994, *MNRAS*, 268, 276
- Willacy, K., Langer, W. D., & Velusamy, T. 1998, *ApJ*, 507, L171

## Appendix A: DCO<sup>+</sup>–H<sub>2</sub> collisional coefficients

Hyperfine-resolved DCO<sup>+</sup>–He rate coefficients have been published recently by Buffa (2012). It is generally assumed that rate coefficients with He multiplied by a factor of 1.4 can provide an estimate of rate coefficients with H<sub>2</sub> ( $J = 0$ ) (Lique et al. 2008). However, for a molecular ion like DCO<sup>+</sup>, this approximation may be invalid, since the electrostatic interaction of an ion with H<sub>2</sub> differs significantly from that with He. We have thus decided to determine hyperfine DCO<sup>+</sup>–H<sub>2</sub> rate coefficients from close coupling (CC) HCO<sup>+</sup>–H<sub>2</sub> rate coefficients ( $k_{J \rightarrow J'}^{CC}(T)$ ) of Flower (1999) using the Infinite order sudden (IOS) approximation described in Faure & Lique (2012). Here, the isotopic substitution of HCO<sup>+</sup> has been ignored since it is expected to have a little impact on the magnitude of the rate coefficients (Buffa 2012).

In DCO<sup>+</sup>, the coupling between the nuclear spin ( $I = 1$ ) of the deuterium atom and the molecular rotation results in a weak splitting (Alexander & Dagdigan 1985) of each rotational level  $J$ , into three hyperfine levels (except for the  $J = 0$  level which is split into only 1 level). Each hyperfine level is designated by a quantum number  $F$  ( $F = I + J$ ) varying between  $|I - J|$  and  $I + J$ .

Within the IOS approximation, inelastic rotational rate coefficients  $k_{J \rightarrow J'}^{IOS}(T)$  can be calculated from the “fundamental” rates (those out of the lowest  $J = 0$  level) as follows (e.g. Corey & McCourt 1983):

$$k_{J \rightarrow J'}^{IOS}(T) = (2J' + 1) \sum_L \begin{pmatrix} J' & J & L \\ 0 & 0 & 0 \end{pmatrix}^2 k_{0 \rightarrow L}^{IOS}(T). \quad (\text{A.1})$$

Similarly, IOS rate coefficients among hyperfine structure levels can be obtained from the  $k_{0 \rightarrow L}^{IOS}(T)$  rate coefficients using the following formula (e.g. Corey & McCourt 1983):

$$k_{JF \rightarrow J'F'}^{IOS}(T) = (2J + 1)(2J' + 1)(2F' + 1) \sum_L \begin{pmatrix} J' & J & L \\ 0 & 0 & 0 \end{pmatrix}^2 \times \left\{ \begin{matrix} J & J' & L \\ F' & F & I \end{matrix} \right\}^2 k_{0 \rightarrow L}^{IOS}(T) \quad (\text{A.2})$$

where  $\begin{pmatrix} \end{pmatrix}$  and  $\left\{ \begin{matrix} \end{matrix} \right\}$  are respectively the “3-j” and “6-j” Wigner symbols.

The IOS approximation is expected to be inaccurate at low temperature. However, it is also expected to correctly predict the relative rates among hyperfine levels within a rotational  $J \rightarrow J'$  transition. Propensity rules are indeed properly included through the Wigner coefficients. As a result, Neufeld & Green (1994) have suggested to compute the hyperfine rates as

$$k_{JF \rightarrow J'F'}^{INF}(T) = \frac{k_{JF \rightarrow J'F'}^{IOS}(T)}{k_{J \rightarrow J'}^{IOS}(T)} k_{J \rightarrow J'}^{CC}(T), \quad (\text{A.3})$$

using the CC rate coefficients  $k^{CC}(0 \rightarrow L)$  of Flower (1999) for the IOS “fundamental” rates ( $k_{J \rightarrow J'}^{IOS}(T)$ ) in Eqs. A.1–A.2.

In addition, the fundamental excitation rates  $k_{0 \rightarrow L}^{CC}$  were replaced by the fundamental de-excitation rates using the detailed balance relation:

$$k_{0 \rightarrow L}^{CC} = (2L + 1)k_{L \rightarrow 0}^{CC}. \quad (\text{A.4})$$

This procedure is found to significantly improve the results at low temperature due to important threshold effects.

Then, from the HCO<sup>+</sup>–H<sub>2</sub> rotational rate coefficients of Flower (1999), we have determined the IOS DCO<sup>+</sup>–H<sub>2</sub> hyperfine rate coefficients using the computational scheme described above. The complete set of (de-)excitation rate coefficients is available online from the LAMDA<sup>1</sup> and BASECOL<sup>2</sup> websites. The present approach has been shown to be accurate, even at low temperature, and has also been shown to induce almost no consequence on the radiative transfer modeling compared to a more exact calculation of the DCO<sup>+</sup>–H<sub>2</sub> rate coefficients (Faure & Lique 2012). However, we note that with the present approach, some hyperfine rate coefficients (those from the  $J = 1, F = 0$  level to a  $J = F$  level) are strictly zero. This selection rule is explained by the “3-j” and “6-j” Wigner symbols that vanish for these kinds of transitions. Using a more accurate approach, these rate coefficients will not be strictly zero but will generally be smaller than the other rates. In addition, Faure & Lique (2012) have shown that it should imply almost no consequences for astrophysical modeling.

<sup>1</sup> LAMDA : <http://www.strw.leidenuniv.nl/moldata/>

<sup>2</sup> BASECOL : <http://basecol.obsmpm.fr/>